Review Article

# Diffusion weighted imaging of the prostate—principles, application, and advances

**Martin H. Maurer, Johannes T. Heverhagen**

Department of Radiology, Inselspital, Bern University Hospital, University of Bern, Bern 3010, Switzerland

*Contributions:* (I) Conception and design: MH Maurer; (II) Administrative support: None; (III) Provision of study materials or patients: MH Maurer; (IV) Collection and assembly of data: MH Maurer; (V) Data analysis and interpretation: MH Maurer; (VI) Manuscript writing: All authors; (VII) Final approval of manuscript: All authors.

*Correspondence to:* Martin H. Maurer, MD. Department of Radiology, Inselspital, Bern University Hospital, University of Bern, Freiburgstrasse 10, Bern 3010, Switzerland. Email: martin.maurer@insel.ch.

**Abstract:** This review article aims to provide an overview on the principles of diffusion-weighted magnetic resonance imaging (DW-MRI) and its applications in the imaging of the prostate. DW-MRI with regards to different applications for prostate cancer (PCa) detection and characterization, local staging as well as for active surveillance (AS) and tumor recurrence after radical prostatectomy (RP) will be discussed. Furthermore, advances in DW-MRI techniques like diffusion kurtosis imaging (DKI) will be presented.

**Keywords:** Magnetic resonance imaging (MRI); diffusion-weighted imaging (DW imaging); prostate cancer (PCa); tumor recurrence; diffusion kurtosis imaging (DKI)

Submitted Apr 17, 2017. Accepted for publication Apr 18, 2017.
doi: 10.21037/tau.2017.05.06
**View this article at:** http://dx.doi.org/10.21037/tau.2017.05.06

## Introduction

The prostate is a reproductive gland in men with a small walnut-like size, however, it becomes very important throughout a men's life as prostate cancer (PCa) was the second most common newly diagnosed type of cancer worldwide in 2012 (1). In the last decade, there has been growing interest in magnetic resonance imaging (MRI) of the prostate as new imaging techniques like diffusion-weighted MRI (DW-MRI) and dynamic contrast-enhanced (DCE) imaging emerged which are now combined with conventional T1- and T2-weighted (T1w and T2w) imaging to multiparametric MRI (mpMRI) protocols of the prostate (2,3). DWI has currently gained the most attention as it allows an accurate localization of malignant foci in the prostate and has a potential role in assessing tumor aggressiveness noninvasively (4-6). This review gives an overview on recent applications of DWI in imaging the prostate and will discuss advances in DW imaging techniques.

## Principles of DW-MRI with regard to the prostate

MRI is based on the signal from hydrogen ($^{1}$H). In DW-MRI the spontaneous mobility of water molecules is measured on a microscopic scale. This mobility is termed Brownian motion and highly relies on the cellular environment of water. DW-MRI therefore reflects abnormalities in different biologic tissues. The degree of motion of water molecules is termed diffusion. As diffusion is mostly restricted by cell membranes, the extent of restriction of free motion is proportionate to the cellular density of a tissue.

DW-MRI most commonly relies on single-shot echo-planar-imaging spin-echo sequences with an application of two rectangular gradient pulses of an equal strength that are applied before and after an 180° refocusing pulse (7,8). In substances with free moving of water molecules, the random movement and displacement between the two pulses will lead to an uncomplete rephrasing by the second pulse and thus leads to a signal loss in DWI that correlates with the

degree of water mobility. Water molecules that do not move undergo a dephasing by the first pulse and are completely rephrased by the second pulse resulting in a high signal (9). The strength of the gradient pulses is expressed by the *b*-value of the DWI sequence. Although an acquisition of at least two *b*-values allows the calculation of apparent diffusion coefficient (ADC) maps, usually three *b*-values are obtained in clinical practice, one low (e.g., 50 s/mm$^2$), one intermediate (e.g., 400 s/mm$^2$) and one high value (e.g., 1,000 s/mm$^2$). In areas with densely packed tumor cells, diffusion is impeded, appearing bright on DW-MRI and darker on the ADC map during visual qualitative assessment of the images (10). Besides a qualitative analysis also a quantitative assessment can be performed by drawing a region of interest (ROI) within a tissue area of interest and then using summary statistics like the mean value within the ROI.

## Recent applications for DW imaging of the prostate

The employment of DWI as a part of a mpMRI protocol has been studied extensively on different aspects of imaging PCa, thereof detection and localization of malignant prostate lesions, characterization and tumor grading, local tumor staging, active surveillance (AS) of already known tumors, and for the evaluation of a response under treatment.

### *Tumor detection*

Initially, the mean ADC value was shown to be significantly lower in tumor tissue than in benign areas of the prostate (11), a finding that was later confirmed by multiple other studies (12-16). Various studies analyzed the additional value of DWI-MRI with conventional T2w imaging and found that both sensitivity (range, 71–89%) and specificity (range, 61–91%) increased significantly when DWI-MRI was combined with T2w imaging, compared with the sole use of T2w imaging (sensitivity, 49–88%; specificity, 57–84%) (13,17-19). The result was confirmed in a recent meta-analysis including ten different studies comparing DW-MRI combined with T2w imaging and T2w imaging alone (sensitivity, 0.72 *vs.* 0.62; specificity 0.81 *vs.* 0.77) (20). Another meta-analysis evaluated the sole use of DW-MRI to detect PCa combining the results of 21 studies and found a high pooled specificity of 0.90 but a relatively low overall pooled sensitivity of only 0.62 (21). This relatively low sensitivity in tumor detection obviously was due to the fact that many studies did not differentiate between tumor detection in the peripheral zone (PZ) and the transition zone (TZ) of the prostate, though DW-MRI is much more sensitive in the PZ than in TZ, where differentiation between common benign hyperplastic nodules and malignant lesions is difficult (22).

With regard to the *b*-values that would provide the most sensitive tumor detection, Metens *et al.* detected the highest tumor visibility using b-values of 1,500 and 2,000 s/mm$^2$ and the best contrast-to-noise ratio (CNR) for b=1,500 s/mm$^2$ using 3 Tesla MRI (23). These results were confirmed by Katahira *et al.* (24) who found the highest specificity (73.2%), specificity (89.7%) and accuracy (84.2%) for PCa detection when using *b*-values of 2,000 s/mm$^2$ in addition to T2w imaging. Similar results were found in a subsequent study by Rosenkrantz *et al.* (25). However, as *b*-values between 1,500 and 2,500 s/mm$^2$ were revealed to be optimal for PCa detection, even higher *b*-values up to 5,000 s/mm$^2$ were not useful and exhibited an overall lower performance in tumor detection (26).

### *Characterization and tumor grading*

Several studies analyzed the value of DW-MRI in addition to conventional T2w imaging with regard to the grading of tumors and their aggressiveness (27,28). In 110 patients with a total of 197 tumors, Verma *et al.* found that the ADC value was negatively correlated with the Gleason score (r=–0.39 for cancers in the PZ). Also in the PZ, higher ADC values were associated with lower Gleason scores. Furthermore, there was no association between ADC value and cancer lesions in the TZ (29). Vargas *et al.* found in 51 patients that a lower mean ADC was significantly associated with a higher Gleason score as the mean ADCs of 1.21, 1.10, 0.87, and 0.69×10$^{-3}$ mm$^2$/sec were associated with a Gleason score of 3+3, 3+4, 4+3, and 8 or higher, respectively (P=0.017) (30). Analyzing a limited patient population of 22 patients with PCas with a median Gleason score of 7 (range, 6–9), Lebovici *et al.* evaluated an intra-patient-normalized ADC ratio between normal tissue and malignant lesions and revealed that these ratios presented significantly lower values in high-risk tumors compared with low-risk tumors both in the central zone (CZ) and the PZ (P<0.001) and had a better diagnostic performance (CZ: AUC, 0.77; sensitivity, 82.2%; specificity, 66.7%; and PZ: AUC, 0.90; sensitivity, 93.7%; specificity, 80%) than stand-alone tumor ADCs (AUC, 0.75; sensitivity, 72.7%; specificity, 70.6%) to

 

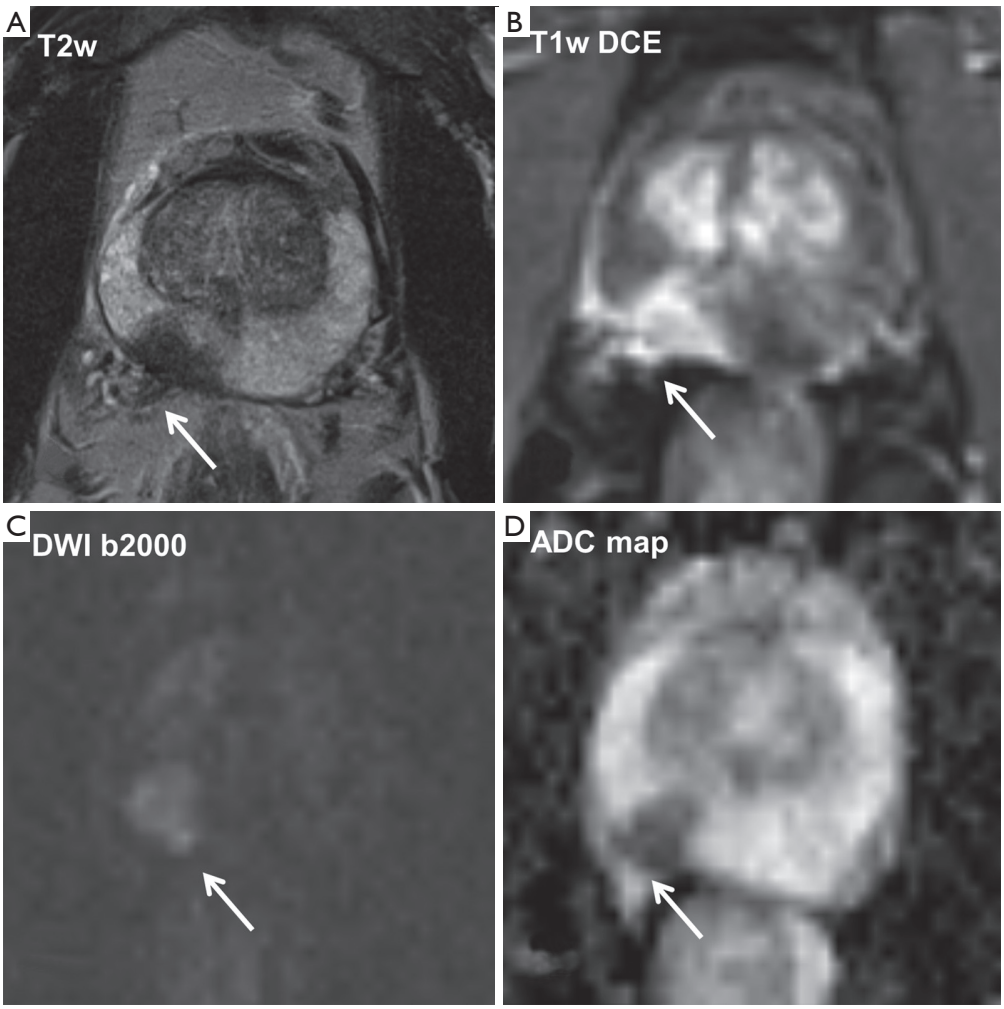


**Figure 1** Multiparametric MRI of the prostate of a 64-year-old patient with a suspicious finding in the right prostate lobe in the rectal digital examination and an elevated PSA level (12 ng/mL). In the midlevel in the right peripheral zone there is a circumscribed T2-weighted (T2w) hypointense lesion with a size of about 14 mm × 10 mm. At its posterior rim the contour of the capsule is discontinuous with infiltration of the adjacent neurovascular bundle with contrast enhancing small nodular tumor tissue (A and B, white arrow). The corresponding area shows a high signal in DW-MRI at a *b*-value of 2,000 s/mm$^2$ (C, white arrow) and a significantly lower ADC value of 0.49×10$^{-3}$ mm$^2$/s compared with about 1.35×10$^{-3}$ mm$^2$/s in other parts of the peripheral zone (D, white arrow). DW-MRI, diffusion-weighted magnetic resonance imaging; ADC, apparent diffusion coefficient.

identify high-risk lesions (31).

### *Local tumor staging*

The local staging of PCa includes a statement on the existence of a capsule infiltration, a possible extracapsular extension (ECE), or infiltration in neighboring structures like the seminal vesicles, the neurovascular bundle or the rectum as well as an invasion of pelvic lymph nodes as all these characteristics are major prognostic factors (32) (see also example in *Figure 1*).

T2w imaging has a high spatial resolution and therefore usually allows a proper evaluation of an infiltration of the prostate capsule or an extracapsular tumor growth. In this context, in a group of 40 patients, thereof 23 had an ECE of PCa, it was shown that DWI and ADC mapping significantly improved the accuracy for preoperative detection of extracapsular growth when added to

 

conventional T2w imaging (P<0.05 for 2 readers) and furthermore increased the positive and negative predictive values for both readers (33). A recent study by Giganti *et al.* including 70 patients developed nomograms to predict ECE of tumors and found that ADC presents a potential biomarker to predict side-specific ECE (34). A study on 166 patients showed that DW-MRI in combination with T2w imaging compared with the sole use of T2w imaging was significantly improving both specificity (from 87% to 97%) and accuracy (from 87% to 96%) for the prediction of an invasion of the seminal vesicles (35). A further study on 283 patients of whom 39 had a tumorous seminal vesicle infiltration revealed that ADC values in seminal vesicles with tumor involvement were significantly lower than those of seminal vesicles that were free of tumor (AUC of T2w combined with DW-MRI, 0.897 versus AUC of T2w imaging alone, 0.779; P<0.05) (36).

### *AS*

Due to a wide-spread use of PSA testing to screen for PCa, there has been a dramatic increase in the incidence of low-risk cancers (37,38). However, a majority of these patients will not die of PCa (39). As a large percentage of these men are treated with either radical prostatectomy (RP) or radiation therapy, there is a vast overtreatment caused by an over-diagnosis of low-risk PCa (40).

As a consequence, AS has emerged as a treatment option for patients with low-risk PCa including regular measurements of PSA levels, digital rectal examinations, and repeat biopsies (41,42). The primary goal of the AS option is to minimize overtreatment while concurrently identifying patients initially diagnosed with low-risk cancer types that have a high-risk disease that was mistaken at the initial assessment or developed it over time after being included in an AS scheme. In this context, a major concern is a misplacement of patients in a low-risk group that actually have a high-grade lesion in the anterior stroma (AS) that was missed with TRUS biopsy (43).

However, regular follow-ups also including TRUS-guided biopsies are expensive. Although significant cost savings are possible over a time period of 10 years comparing AS programs with upfront interventions (44), there is also a relevant percentage of patients under AS that are reclassified over time and then undergo surgery of radiation therapy increasing the costs compared with an upfront intervention (42,45). Furthermore, biopsies always underlie a risk of adverse events as up to 25% of patients have transient symptoms of the lower urinary tract after a biopsy and a not negligible percentage of men develop a febrile prostatitis (46-48). In contrast, AS based solely on PSA kinetics was shown to be insufficient (49).

In this context, mpMRI including DWI has gained attention as a possible tool to identify clinically significant cancer in the entire gland, and to perceive and monitor patients treated with AS (50,51). For a proper patient selection and detecting significant PCa with mpMRI before diagnostic biopsy in men with abnormal PSA levels or abnormal digital rectal examination, Thompson *et al.* (52) revealed for mpMRI that the negative predictive value of identifying clinically significant cancer was 100% for high-risk patients and 96% for low-risk patients while the positive predictive value was 71% for high-risk and 28% for low-risk patients. For patients under AS, there is the concern that the histological tumor grade might worsen in the course of time. Bonekamp *et al.* analyzed the predictive value of mpMRI compared with clinical parameters for reclassification in a group of 50 men (53). They found that mpMRI best predicted disease reclassification in patients who did not meet clinical AS enrollment criteria and had a suspicious lesion 10 mm or greater and concluded that mpMRI had incremental predictive value when used in combination with clinical AS enrollment criteria.

### *Detection of tumor recurrence after RP*

In patients with a localized PCa, RP is the most common primary treatment. However, in the time interval of 10 years there is a significant incidence of up to 30% for a biochemical recurrence (BCR) following RP (54). However, a BCR can precede a tumor recurrence that can be diagnosed with imaging methods by up to 10 years (55). After a RP, recurrent disease is most commonly found in the prostate fossa and in pelvic and retroperitoneal lymph nodes (56,57). MRI was shown to be superior to other imaging modalities like TRUS, CT and also $^{11}$C-choline-PET-CT having a sensitivity of 83% to 95% to detect local tumor recurrence (58,59). Recent studies have revealed that DCE imaging has very high sensitivities of 97–100% and specificities of up to 97% detecting recurrent cancer (60,61). However, other studies focusing on DWI showed that DWI alone can be a reliable method to detect local recurrence with a sensitivity and specificity of up to 98% and 96%, respectively (60,62) (see also example in *Figure 2*).

 

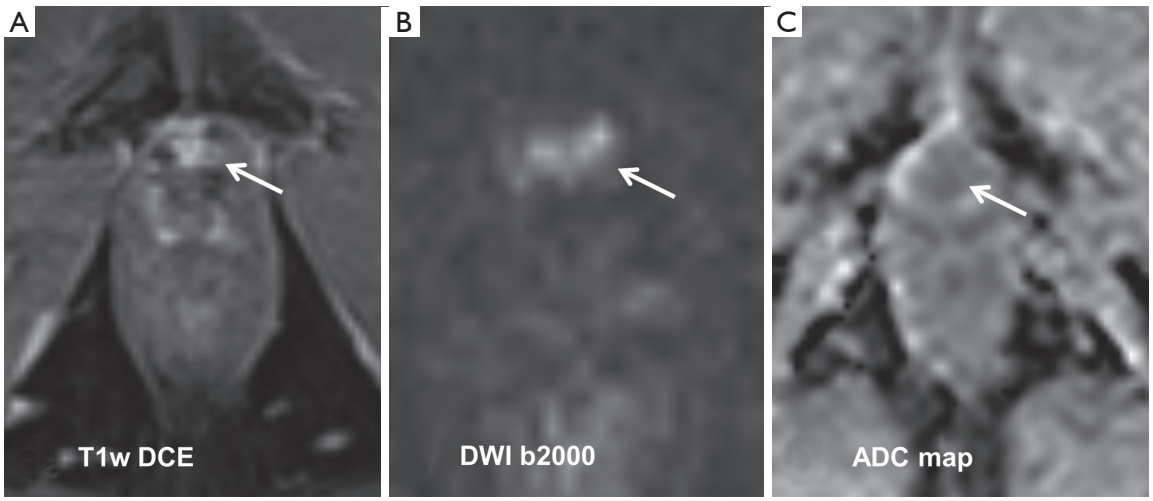


**Figure 2** A 62-year-old patient that underwent radical prostatectomy and radiation therapy 5 years ago now showing an elevated PSA level (16 ng/mL). The dynamic contrast enhanced T1-weighted (T1w) sequence reveals a small lesion with a size of 10 mm × 8 mm close to the anterior vesicourethral anastomosis (A, white arrow). In DW-MRI, the same lesion shows a high signal at a *b*-value of 2,000 s/mm$^2$ and a corresponding low signal in the ADC map (B and C, white arrows) confirming a recurrent tumor with densely packed tumor cells. DW-MRI, diffusion-weighted magnetic resonance imaging; ADC, apparent diffusion coefficient.

## Advances in DWI of the prostate

### *Kurtosis imaging*

The standard monoexponential estimation of ADC assumes a Gaussian distribution of the displacement of water molecules within an analyzed tissue. However, water diffusion usually is restricted in human tissues due to microstructural barriers like cellular membranes. The concept of diffusion kurtosis imaging (DKI) was first described by Jensen *et al.* in 2005 where the term kurtosis stands for the extent of deviation of a non-Gaussian from a standard Gaussian distribution being measured in a dimensionless quantity (K) (63). DKI is thought to better reflect the influence of the microstructural complexity in normal and tumor tissue with a different tumor grading than standard DWI. Diffusion kurtosis can be extracted from DWI but requires high *b*-values of about 2,000–3,000 s/mm$^2$ to quantify the deviation of tissue diffusion from a usual Gaussian pattern.

So far, several studies have investigated the value of DKI compared with standard DWI with regard to assess the aggressiveness of PCa. However, the results have been inconsistent with studies that observed a better performance of DKI (64-66) while others did not confirm an additional benefit (67,68).

On the one hand, Rosenkrantz *et al.* (64) found in 47 patients with biopsy-proven PCa that K values were significantly higher both in cancer areas compared with benign areas of the PZ (0.96±0.24 *vs.* 0.57±0.07; P<0.001) as well as in tumor areas with higher rather than lower Gleason scores (1.05±0.26 *vs.* 0.89±0.20). Furthermore, DKI showed a significantly greater sensitivity than ADC for differentiating cancerous areas from benign areas in the PZ (93.3% *vs.* 78.5%; P<0.001) with equal specificity (95.7%; P>0.99). On the other hand, Roethke *et al.* did not confirm these results in a patient group of 55 patients (67). Although K was significantly higher in areas with proven cancer than in benign tissue (1.01±0.21 *vs.* 0.76±0.14; P<0.05), receiver operating characteristic (ROC) analysis did not show a significant difference between DKI and ADC for detecting tumor tissue. Regarding tumor aggressiveness K and standard ADC showed a comparable significant difference to differentiate between high- and low-grade tumors. One possible explanation for the discrepancy between these studies could be the way ADC was calculated. Rosenkrantz *et al.* (69) calculated the ADC from the DW-kurtosis sequence which has an increased echo time to allow high *b*-values necessary for this sequence. However, longer echo times may decrease the signal-to-noise ratio (SNR) with a negative impact on the ADC map that may lead to an overestimation of the value of DKI compared with ADC. This goes along with the results of Roethke *et al.* (67) who

 

did not find a significant benefit of DKI compared with ADC as they used a separate DWI sequence with shorter echo times and lower *b*-values to calculate ADC maps. Recently, a study comparing the value of DW-MRI and DKI for PCa detection and characterization included a large population of 255 patients to evaluate the potential value of DKI (70). The authors found that ADC and DKI were highly correlated and had a similar diagnostic performance, but did not show a clear added value of DKI compared with standard DW-MRI. Therefore, the value of additional DKI remains unclear and it is questionable if it should be incorporated into routine clinical imaging.

## Summary and conclusions

As a part of a mpMRI protocol, DW-MRI covers a wide range of applications in imaging of the prostate and was shown to give useful additional information with regard to tumor detection and characterization, evaluation of tumor recurrence after RP and in risk stratifying of low-risk tumor patients under AS. The benefit of additional imaging techniques like DKI is still unclear and needs further evaluation.

## Acknowledgements

None.

## Footnote

*Conflicts of Interest*: The authors have no conflicts of interest to declare.

## References

1. Torre LA, Bray F, Siegel RL, et al. Global cancer statistics, 2012. CA Cancer J Clin 2015;65:87-108.
2. Johnson LM, Turkbey B, Figg WD, et al. Multiparametric MRI in prostate cancer management. Nat Rev Clin Oncol 2014;11:346-53.
3. Hoeks CM, Barentsz JO, Hambrock T, et al. Prostate cancer: multiparametric Mr imaging for detection, localization, and staging. Radiology 2011;261:46-66.
4. Ueno Y, Tamada T, Bist V, et al. Multiparametric magnetic resonance imaging: Current role in prostate cancer management. Int J Urol 2016;23:550-7.
5. Scheenen TW, Rosenkrantz AB, Haider MA, et al. Multiparametric magnetic resonance imaging in prostate cancer management: current status and future perspectives. Invest Radiol 2015;50:594-600.
6. Vos EK, Kobus T, Litjens GJ, et al. Multiparametric Magnetic Resonance Imaging for Discriminating Low-Grade From High-Grade Prostate Cancer. Invest Radiol 2015;50:490-7.
7. Le Bihan D, Breton E, Lallemand D, et al. Mr imaging of intravoxel incoherent motions: application to diffusion and perfusion in neurologic disorders. Radiology 1986;161:401-7.
8. Neil JJ. Diffusion imaging concepts for clinicians. J Magn Reson Imaging 2008;27:1-7.
9. Koh DM, Collins DJ. Diffusion-weighted MRI in the body: applications and challenges in oncology. AJR Am J Roentgenol 2007;188:1622-35.
10. Charles-Edwards EM, deSouza NM. Diffusion-weighted magnetic resonance imaging and its application to cancer. Cancer Imaging 2006;6:135-43.
11. Issa B. In vivo measurement of the apparent diffusion coefficient in normal and malignant prostatic tissues using echo-planar imaging. J Magn Reson Imaging 2002;16:196-200.
12. Sato C, Naganawa S, Nakamura T, et al. Differentiation of noncancerous tissue and cancer lesions by apparent diffusion coefficient values in transition and peripheral zones of the prostate. J Magn Reson Imaging 2005;21:258-62.
13. Gibbs P, Pickles MD, Turnbull LW. Diffusion imaging of the prostate at 3.0 tesla. Invest Radiol 2006;41:185-8.
14. Pickles MD, Gibbs P, Sreenivas M, et al. Diffusion-weighted imaging of normal and malignant prostate tissue at 3.0T. J Magn Reson Imaging 2006;23:130-4.
15. Kim CK, Park BK, Han JJ, et al. Diffusion-weighted imaging of the prostate at 3 T for differentiation of malignant and benign tissue in transition and peripheral zones: preliminary results. J Comput Assist Tomogr 2007;31:449-54.
16. Tamada T, Sone T, Jo Y, et al. Apparent diffusion coefficient values in peripheral and transition zones of the prostate: comparison between normal and malignant prostatic tissues and correlation with histologic grade. J Magn Reson Imaging 2008;28:720-6.
17. Miao H, Fukatsu H, Ishigaki T. Prostate cancer detection with 3-T MRI: comparison of diffusion-weighted and T2-weighted imaging. Eur J Radiol 2007;61:297-302.
18. Haider MA, van der Kwast TH, Tanguay J, et al. Combined T2-weighted and diffusion-weighted MRI for localization of prostate cancer. AJR Am J Roentgenol

 

2007;189:323-8.
19. Lim HK, Kim JK, Kim KA, et al. Prostate cancer: apparent diffusion coefficient map with T2-weighted images for detection--a multireader study. Radiology 2009;250:145-51.
20. Wu LM, Xu JR, Ye YQ, et al. The clinical value of diffusion-weighted imaging in combination with T2-weighted imaging in diagnosing prostate carcinoma: a systematic review and meta-analysis. AJR Am J Roentgenol 2012;199:103-10.
21. Chen J, Liu RB, Tan P. The value of diffusion-weighted imaging in the detection of prostate cancer: a meta-analysis. Eur Radiol 2014;24:1929-41.
22. Oto A, Kayhan A, Jiang Y, et al. Prostate cancer: differentiation of central gland cancer from benign prostatic hyperplasia by using diffusion-weighted and dynamic contrast-enhanced Mr imaging. Radiology 2010;257:715-23.
23. Metens T, Miranda D, Absil J, et al. What is the optimal b value in diffusion-weighted MR imaging to depict prostate cancer at 3T? Eur Radiol 2012;22:703-9.
24. Katahira K, Takahara T, Kwee TC, et al. Ultra-high-b-value diffusion-weighted Mr imaging for the detection of prostate cancer: evaluation in 201 cases with histopathological correlation. Eur Radiol 2011;21:188-96.
25. Rosenkrantz AB, Hindman N, Lim RP, et al. Diffusion-weighted imaging of the prostate: Comparison of b1000 and b2000 image sets for index lesion detection. J Magn Reson Imaging 2013;38:694-700.
26. Rosenkrantz AB, Parikh N, Kierans AS, et al. Prostate cancer detection using computed very high b-value diffusion-weighted imaging: how high should we go? Acad Radiol 2016;23:704-11.
27. Hambrock T, Hoeks C, Hulsbergen-van de Kaa C, et al. Prospective assessment of prostate cancer aggressiveness using 3-T diffusion-weighted magnetic resonance imaging-guided biopsies versus a systematic 10-core transrectal ultrasound prostate biopsy cohort. Eur Urol 2012;61:177-84.
28. Desouza NM, Riches SF, Vanas NJ, et al. Diffusion-weighted magnetic resonance imaging: a potential non-invasive marker of tumour aggressiveness in localized prostate cancer. Clin Radiol 2008;63:774-82.
29. Verma S, Rajesh A, Morales H, et al. Assessment of aggressiveness of prostate cancer: correlation of apparent diffusion coefficient with histologic grade after radical prostatectomy. AJR Am J Roentgenol 2011;196:374-81.
30. Vargas HA, Akin O, Franiel T, et al. Diffusion-weighted endorectal Mr imaging at 3 T for prostate cancer: tumor detection and assessment of aggressiveness. Radiology 2011;259:775-84.
31. Lebovici A, Sfrangeu SA, Feier D, et al. Evaluation of the normal-to-diseased apparent diffusion coefficient ratio as an indicator of prostate cancer aggressiveness. BMC Med Imaging 2014;14:15.
32. Eggener SE, Scardino PT, Walsh PC, et al. Predicting 15-Year prostate cancer specific mortality after radical prostatectomy. J Urol 2011;185:869-75.
33. Lawrence EM, Gallagher F, Barrett T, et al. Preoperative 3-T diffusion-weighted MRI for the qualitative and quantitative assessment of extracapsular extension in patients with intermediate-or high-risk prostate cancer. AJR Am J Roentgenol 2014;203:W280-6.
34. Giganti F, Coppola A, Ambrosi A, et al. Apparent diffusion coefficient in the evaluation of side-specific extracapsular extension in prostate cancer: Development and external validation of a nomogram of clinical use. Urol Oncol 2016;34:291.e9-291.e17.
35. Kim CK, Choi D, Park BK, et al. Diffusion-weighted Mr imaging for the evaluation of seminal vesicle invasion in prostate cancer: initial results. J Magn Reson Imaging 2008;28:963-9.
36. Ren J, Huan Y, Wang H, et al. Seminal vesicle invasion in prostate cancer: prediction with combined T2-weighted and diffusion-weighted Mr imaging. Eur Radiol 2009;19:2481-6.
37. Weir HK, Thun MJ, Hankey BF, et al. Annual report to the nation on the status of cancer, 1975-2000, featuring the uses of surveillance data for cancer prevention and control. J Natl Cancer Inst 2003;95:1276-99.
38. Cooperberg MR, Lubeck DP, Meng MV, et al. The changing face of low-risk prostate cancer: trends in clinical presentation and primary management. J Clin Oncol 2004;22:2141-9.
39. Rider JR, Sandin F, Andrén O, et al. Long-term outcomes among noncuratively treated men according to prostate cancer risk category in a nationwide, population-based study. Eur Urol 2013;63:88-96.
40. Welch HG, Black WC. Overdiagnosis in cancer. J Natl Cancer Inst 2010;102:605-13.
41. Heidenreich A, Bastian PJ, Bellmunt J, et al. EAU guidelines on prostate cancer. part 1: screening, diagnosis, and local treatment with curative intent-update 2013. Eur Urol 2014;65:124-37.
42. Klotz L, Zhang L, Lam A, et al. Clinical results of long-term follow-up of a large, active surveillance cohort with localized prostate cancer. J Clin Oncol 2010;28:126-31.

 

43. Lawrentschuk N, Haider MA, Daljeet N, et al. 'Prostatic evasive anterior tumours': the role of magnetic resonance imaging. BJU Int 2010;105:1231-6.
44. Keegan KA, Dall'Era MA, Durbin-Johnson B, et al. Active surveillance for prostate cancer compared with immediate treatment: an economic analysis. Cancer 2012;118:3512-8.
45. Tosoian JJ, Trock BJ, Landis P, et al. Active surveillance program for prostate cancer: an update of the Johns Hopkins experience. J Clin Oncol 2011;29:2185-90.
46. Loeb S, Vellekoop A, Ahmed HU, et al. Systematic review of complications of prostate biopsy. Eur Urol 2013;64:876-92.
47. Loeb S, Carter HB, Berndt SI, et al. Is repeat prostate biopsy associated with a greater risk of hospitalization? Data from SEER-Medicare. J Urol 2013;189:867-70.
48. Loeb S, Carter HB, Berndt SI, et al. Complications after prostate biopsy: data from SEER-Medicare. J Urol 2011;186:1830-4.
49. Ross AE, Loeb S, Landis P, et al. Prostate-specific antigen kinetics during follow-up are an unreliable trigger for intervention in a prostate cancer surveillance program. J Clin Oncol 2010;28:2810-6.
50. Tseng KS, Landis P, Epstein JI, et al. Risk stratification of men choosing surveillance for low risk prostate cancer. J Urol 2010;183:1779-85.
51. Komai Y, Numao N, Yoshida S, et al. High diagnostic ability of multiparametric magnetic resonance imaging to detect anterior prostate cancer missed by transrectal 12-Core biopsy. J Urol 2013;190:867-73.
52. Thompson JE, Moses D, Shnier R, et al. Multiparametric magnetic resonance imaging guided diagnostic biopsy detects significant prostate cancer and could reduce unnecessary biopsies and over detection: a prospective study. J Urol 2014;192:67-74.
53. Bonekamp D, Bonekamp S, Mullins JK, et al. Multiparametric magnetic resonance imaging characterization of prostate lesions in the active surveillance population: incremental value of magnetic resonance imaging for prediction of disease reclassification. J Comput Assist Tomogr 2013;37:948-56.
54. Freedland SJ, Humphreys EB, Mangold LA, et al. Risk of prostate cancer-specific mortality following biochemical recurrence after radical prostatectomy. JAMA 2005;294:433-9.
55. Pound CR, Partin AW, Eisenberger MA, et al. Natural history of progression after PSA elevation following radical prostatectomy. JAMA 1999;281:1591-7.
56. Mitchell CR, Lowe VJ, Rangel LJ, et al. Operational characteristics of (11)c-choline positron emission tomography/computerized tomography for prostate cancer with biochemical recurrence after initial treatment. J Urol 2013;189:1308-13.
57. Kitajima K, Murphy RC, Nathan MA, et al. Detection of recurrent prostate cancer after radical prostatectomy: comparison of 11C-choline PET/CT with pelvic multiparametric MR imaging with endorectal coil. J Nucl Med 2014;55:223-32.
58. Linder BJ, Kawashima A, Woodrum DA, et al. Early localization of recurrent prostate cancer after prostatectomy by endorectal coil magnetic resonance imaging. Can J Urol 2014;21:7283-9.
59. Alfarone A, Panebianco V, Schillaci O, et al. Comparative analysis of multiparametric magnetic resonance and PET-CT in the management of local recurrence after radical prostatectomy for prostate cancer. Crit Rev Oncol Hematol 2012;84:109-21.
60. Panebianco V, Barchetti F, Sciarra A, et al. Prostate cancer recurrence after radical prostatectomy: the role of 3-T diffusion imaging in multi-parametric magnetic resonance imaging. Eur Radiol 2013;23:1745-52.
61. Roy C, Foudi F, Charton J, et al. Comparative sensitivities of functional MRI sequences in detection of local recurrence of prostate carcinoma after radical prostatectomy or external-beam radiotherapy. AJR Am J Roentgenol 2013;200:W361-8.
62. Cha D, Kim CK, Park SY, et al. Evaluation of suspected soft tissue lesion in the prostate bed after radical prostatectomy using 3T multiparametric magnetic resonance imaging. Magn Reson Imaging 2015;33:407-12.
63. Jensen JH, Helpern JA, Ramani A, et al. Diffusional kurtosis imaging: The quantification of non-Gaussian water diffusion by means of magnetic resonance imaging. Magn Reson Med 2005;53:1432-40.
64. Rosenkrantz AB, Sigmund EE, Johnson G, et al. Prostate cancer: feasibility and preliminary experience of a diffusional kurtosis model for detection and assessment of aggressiveness of peripheral zone cancer. Radiology 2012;264:126-35.
65. Suo S, Chen X, Wu L, et al. Non-Gaussian water diffusion kurtosis imaging of prostate cancer. Magn Reson Imaging 2014;32:421-7.
66. Wang Q, Li H, Yan X, et al. Histogram analysis of diffusion kurtosis magnetic resonance imaging in differentiation of pathologic Gleason grade of prostate cancer. Urol Oncol 2015;33:337.e15-24.
67. Roethke MC, Kuder TA, Kuru TH, et al. Evaluation


 

of diffusion kurtosis imaging versus standard diffusion imaging for detection and grading of peripheral Zone prostate cancer. Invest Radiol 2015;50:483-9.
68. Toivonen J, Merisaari H, Pesola M, et al. Mathematical models for diffusion-weighted imaging of prostate cancer using b values up to 2000 s/mm(2) : correlation with Gleason score and repeatability of region of interest analysis. Magn Reson Med 2015;74:1116-24.
69. Rosenkrantz AB, Mussi TC, Spieler B, et al. High-grade bladder cancer: association of the apparent diffusion coefficient with metastatic disease: preliminary results. J Magn Reson Imaging 2012;35:1478-83.
70. Tamada T, Prabhu V, Li J, et al. Diffusion-weighted MR Imaging for Detection and Assessment of Aggressiveness-Comparison between Conventional and Kurtosis Models. Radiology 2017;284:100-8.

**Cite this article as:** Maurer MH, Heverhagen JT. Diffusion weighted imaging of the prostate—principles, application, and advances. Transl Androl Urol 2017;6(3):490-498. doi: 10.21037/tau.2017.05.06

 